 doi:10.20944/preprints202206.0244.v1

Article

Indicated Role of Small Cellular Particles in Mediating Inter-Species Interaction for Removal of Bisphenols from Conditioned Media

David Škufca [1,†], Darja Božič [1,2,†], Matej Hočevar[3], Marko Jeran[1,2], Apolonija Bedina Zavec[4], Matic Kisovec[4], Marjetka Podobnik[4], Tadeja Matos[5], Rok Tomazin[5], Aleš Iglič[2], Tjaša Griessler Bulc[1], Ester Heath[6,7] and Veronika Kralj-Iglič [1,*]

1. University of Ljubljana, Faculty of Health Sciences, Biomedical Research Group, Ljubljana, Slovenia
2. University of Ljubljana, Faculty of Electrical Engineering, Laboratory of Physics, Ljubljana, Slovenia
3. Institute of Metals and Technology, Department of Physics and Chemistry of Materials, Ljubljana, Slovenia
4. National Institute of Chemistry, Department of Molecular Biology and Nanobiotechnology, Ljubljana, Slovenia
5. University of Ljubljana, Faculty of Medicine, Institute of Microbiology and Immunology, Ljubljana, Slovenia
6. Jožef Stefan Institute, Department of Environmental Sciences, Ljubljana, Slovenia
7. Jožef Stefan International Postgraduate School, Ljubljana, Slovenia

† :Authors contributed equally to this paper.

* Correspondence: veronika.kralj-iglic@fe.uni-lj.si

Abstract: Small cellular particles are released into the surroundings of cells and are proposed to play an important role in intercellular communication and consequently the responses of microbial communities to environmental stressors. We studied the connection between the small cellular particles and the efficiency of three culture series of the microalge *Phaeodactylum tricornutum* and bacteria (axenic microalgae, bacterial culture and co-culture of the two) in removing bisphenols from their growth medium. The microorganism growth rate was determined by flow cytometry, protein profiles were examined by protein gel electrophoresis, cultures and small cellular particle isolates were imaged by scanning electron microscopy, and bisphenols were analyzed using gas chromatography coupled with tandem mass spectrometry (GC-MS/MS). Higher growth rates of microalgae were observed in the co-culture than in the axenic microalgal culture, while the presence of bisphenols neither influenced the morphology of the microalgal cells, protein profiles, nor the small cellular particle isolates. Biotic removal of bisphenols ranged from 0% to 71% and differed among the culture series in a compound-specific manner. However, it remains unclear which mechanisms influenced algal growth and bisphenol removal. Further research on the mechanisms of interspecies communication is needed to advance our understanding of microbial communities at the nano-level.

Keywords: contaminants of emerging concern; bisphenol; microalgae; *Phaeodactylum tricornutum*; bacteria; extracellular vesicles; electron microscopy; flow cytometry; mass spectrometry

1. Introduction

Nature-based solutions for wastewater treatment with their ability for integrated resource management are promising for developing a circular economy in the urban environment [1]. One such example are algal photobioreactors, most notably high rate algal ponds (HRAP), which rely on algae and bacterial communities to treat wastewater and produce biomass [2]. Compared to activated sludge reactors used for treating wastewater, HRAPs have longer hydraulic retention times and a large surface area, i.e., 1 ha or more

 doi:10.20944/preprints202206.0244.v1

in -full-size HRAP systems [2–4]. Also, they do not require active aeration since the algae produce O_2 and organic acids needed by the bacteria, which contribute CO_2 and nutrients for the algae [2]. The main advantage of photobioreactors is the production of nutrient- and energy-rich algal biomass that may be exploited as a feedstock, i.e., for polymer, energy (e.g., biogas or biodiesel) and fertilizer production [5–8]. However, our understanding of nature-based solutions needs to progress from the technological unit level to the cellular community level since cellular communication plays a fundamental role in the homeostasis of complex biological systems where synchronization, cooperation, quick adaptation and specialization/differentiation of the cells occurs [9–11]. It is now acknowledged that cells release various types of cellular particles (SCPs), including extracellular vesicles (EVs), antibody complexes, lipoproteins and other particles capable of transporting different substances, like proteins, lipids, sugars and nucleic acids [12]. EVs have been implicated in many aspects of cell physiology, such as stress response, intercellular competition, lateral gene transfer (via RNA or DNA), pathogenicity, and detoxification [12]. Although microalgal SCPs were first observed in the 1970s [13,14], their roles in communities are not yet fully understood. In this work we have focused on the study of SCPs of *Phaeodactylum tricornutum* (*P. tricornutum*) [15], for it was previously recognized as one of the species with appreciable yields of SCPs in isolates from conditioned media [16,17].

Contaminants of emerging concern (CEC) include active components of human and veterinary pharmaceuticals, illicit drugs, personal care products, pesticides, hormones, flame retardants, plasticizers and other compounds, as well as their metabolites and transformation products (TPs) [18,19]. However, their environmental occurrence and fate have been investigated only recently due to awareness of potential adverse ecological and human health impacts, although CEC may not be new in the environment [20]. CEC are typically present in the environment at trace levels, and only recent advances in analytical instrumentation have allowed their detection at low concentrations (ng/L and even pg/L) [18]. Bisphenols (BPs) are a group of CEC characterized by two hydroxyphenyl groups bound by a hydrocarbon bridge and otherwise containing diverse chemical groups, resulting in different physicochemical properties and consequent environmental behaviour, making them suitable model compounds. Bisphenols are monomers used to produce polycarbonate, epoxy resin, polysulfone, polyacrylate, polyetherimide, and as an additive in thermal paper, polyvinyl chloride, and other products [21], and it was indicated that their emissions into wastewater are not negligible [22]. Studies point toward BPs causing endocrine disruption and other toxic effects, e.g. reproductive toxicity, neurotoxicity and cytotoxicity [23], which is concerning as they may cause ecological harm [24]. Wastewater represents the main influx of CEC to the environment due to inadequate removal during wastewater treatment [2,19,25]. They may also pose a risk to humans when considering reusing treated wastewater products (e.g. reclaimed water and biomass) for activities like agriculture.

Microalgal photobioreactors are an alternative to conventional wastewater treatment [26]. Biodegradation of CEC in microalgal photobioreactors results from the metabolism of microalgae and bacteria, either intracellularly or extracellularly [27]. Co-metabolic biodegradation may be accomplished by non-specific enzymes produced to assimilate other organic compounds [28]. Furthermore, microalgae often grow in co-culture with bacteria [29]. Liu et al. (2021) postulate that biodegradation of CEC may take place according to three scenarios: (1) microalgae do not directly degrade the compound but provide a favourable environment for bacteria, promoting biodegradation, (2) bacteria and microalgae both significantly and directly contribute to the biodegradation of CEC, and (3) microalgae and bacteria synergistically degrade CEC, where one can degrade the intermediate products of the other or vice versa [28]. Past experimental studies have shown that a co-culture of microalgae and bacteria is more efficient at removing organic pollutants than a single culture. Similarly, Ji et al. (2018) show that a co-culture of *Chlorella vulgaris* and *Bacillus licheniformis* reduces chemical oxygen demand, total dissolved nitrogen, and total dissolved phosphorus compared to an axenic culture of microalgae. Additionally, they

 doi:10.20944/preprints202206.0244.v1

report a two-fold higher peak in Chlorophyll *a* values in the co-culture, along with altered expressions of Chlorophyll-related genes [30].

Some bacterial strains in the native phycosphere (mini-ecosystem surrounding microalgal cell walls) may improve the growth of *C. vulgaris* (e.g. *Flavobacterium*, *Hyphomonas*, *Rhizobium* and *Sphingomonas*). In contrast, others may be inhibitory (*Microbacterium* and *Exophiala*), illustrating that not all interactions need to be mutualistic. Kumari et al. (2016) report that a co-culture of *Scenedesmus* sp. and *Paenibacillus* sp. was more successful than either grown axenic in removing organic contaminants, TDS, COD and heavy metals as well as showing the highest reduction in cytotoxicity and genotoxicity [31]. These studies point to interspecies interactions between bacteria and microalgae, which may impact a photobioreactor's performance, although the underlying mechanisms are poorly understood. It is, therefore, of utmost importance to enhance our understanding of intercellular communication mechanisms, and we expect that this would have implications across multiple fields of science [17].

In this work, we focus on SCPs and how they affect the removal of bisphenols from wastewater and test the hypothesis that a co-culture of microalgae and bacteria is more efficient in removing bisphenols than a pure axenic microalgal or bacterial culture. We also assessed microbial growth, the morphology of isolated SCPs, and the concentration of different BPs in the media since we expect BPs to induce protein and SCP changes. Three different *in vitro* cultures were studied: 1) an axenic microalgal culture of the diatom *Phaeodactylum tricornutum*, 2) a co-culture of microalgae and bacteria, and 3) a bacterial culture.

2. Results

Microorganism growth rates were determined by measuring cell concentration in culture samples using flow cytometry (FCM). Isolates of SCPs were prepared by differential centrifugation. Cultures and isolates were examined by protein gel electrophoresis (SDS-PAGE), cryogenic transmission electron microscopy (cryo-TEM) and scanning electron microscopy (SEM) to evaluate possible qualitative differences between samples. BPs were analysed by gas chromatography coupled with tandem mass spectrometry (GC-MS/MS). For one week, the cultures were grown in media supplemented with BPs, and blank cultures (the respective microorganisms in the media without added BP) were grown as controls.

2.1. Culture growth

Cultures are referred to as experimental series (addition of BPs): axenic microalgae (EA), co-culture of microalgae and bacteria (EC) and bacterial culture (EB) and as blank control series (no addition of BPs): axenic microalgae (BA), co-culture of microalgae and bacteria (BC) and bacterial culture (BB), each in triplicate (for details see Table 1). The growth of algal cells in the different cultures was followed by counting events of autofluorescent particles (AFPs) by flow cytometry (FCM), which also sets them apart from non-fluorescent particles (NFPs), that were attributed to bacteria as well as SCPs from bacteria and algae. Both AFPs and NFPs were quantified in all experimental and blank control series to check for possible contamination by microalgae or bacteria. The AFPs and NFPs were defined by the respective regions of the FCM diagrams as described in Figure 8 (Materials and Methods).

Quantification of AFPs shows that the starting concentrations of microalgae cells were approximately 10^6 cells mL^{-1} for the microalgae (Figure 1: EA, BA, EC, BC), while the concentration of AFPs in EA showed a mean microalgal cell concentration of $5.3 \pm 2.8 \times 10^6$ cells mL^{-1} and a similar value of $5.0 \pm 2.2 \times 10^6$ cells mL^{-1} in the respective control (BA) after 168 h (Figure 1). The co-culture EC and respective blank BC reached higher microalgal cell concentrations than axenic the cultures, i.e., $7.6 \pm 1.4 \times 10^6$ cells mL^{-1} and $7.3 \pm 1.7 \times 10^6$ cells mL^{-1}, respectively.

Preprints (www.preprints.org) | NOT PEER-REVIEWED | Posted: 17 June 2022 doi:10.20944/preprints202206.0244.v1

The starting concentration of detected NFPs in the axenic cultures was 2.2×10^5 mL^{-1} in EA and 2.3×10^5 mL^{-1} in BA. NFP concentration increased during the experiment for less than 5.0×10^5 mL^{-1}, an increase attributed to SCPs and cellular debris. The starting concentration of events detected in the same gate in the co-cultures and bacterial cultures was approximately 0.5×10^6 mL^1. Therefore, events detected in this gate in the samples with bacteria present were mainly attributed to the bacterial cells.

After 168 hours, the concentration of NFPs was comparable in the BPs-treated and non-treated replicates: $1.9 \pm 0.2 \times 10^6$ mL^{-1} in the EC and $2.0 \pm 0.1 \times 10^6$ mL^{-1} in BC and $8.0 \pm 0.6 \times 10^6$ cells mL^{-1}in experimental bacterial cultures (EB) and $10.3 \pm 2.0 \times 10^6$ cells mL^{-1} the blank bacterial cultures (BB). In these cultures, the concentration of NFPs increased up to 72 h and then declined slightly until 168 h. The maximum concentration (measured at 72 h) was $3.6 \pm 0.7 \times 10^6$ mL^{-1} and $2.8 \pm 0.2 \times 10^6$ mL^{-1}, in EC and BC, respectively, and $10.3 \pm 0.4 \times 10^6$ mL^{-1} and $10.6 \pm 1.1 \times 10^6$ mL^{-1}, in EB and BB, respectively (Figure 1).

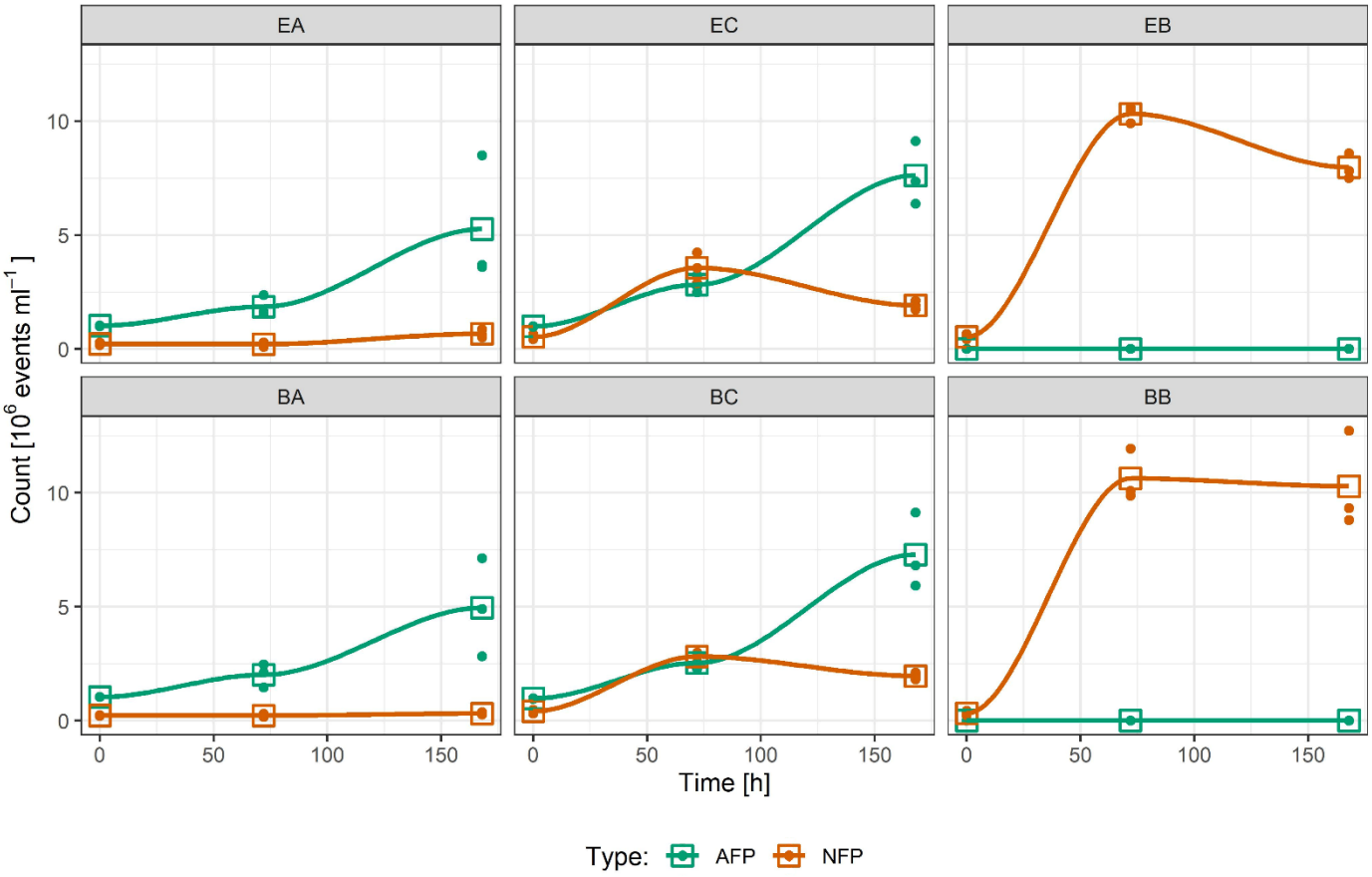

Figure 1. Plots showing growth of cultures, presented by autofluorescent particles (i.e. microalgae) (AFPs) and non-fluorescent particles (NFPs), including bacteria and SCPs, measured by flow cytometer. Single observations are shown as dots, while the mean value of three replicates is presented as an empty square.

To check the presence of bacteria in the samples, the cultures were inoculated onto the MW-LB-agar plates. No bacterial growth was detected in the axenic microalgal samples, while smooth beige colonies grew in the co-culture and bacterial samples. In the co-cultures, no zone of inhibition was observed between microalgae and bacteria, and microalgal growth was centred in the centre of the bacterial mat (Figure A3).

2.2. Cell morphology, protein profile and nanoparticle characterization

 doi:10.20944/preprints202206.0244.v1

In microalgae-containing samples, *P. tricornuum* was mainly in the fusiform shape (Figure 2: EA, BA, EC, BC). Monotrichous bacteria were observed in co-culture and bacterial samples (Figure 2: EC, BC, EB, BB). Also, bacterial cells with other distinct morphologies were observed, such as rod-shaped cells with a rough-hairy surface (Figure 2: EB, BB) and drill-shaped cells (Figure 2: EC, BB). A larger number of the latter were observed with SEM in the samples of co-cultures than in bacterial samples (not shown). We observed no effects of BPs on the morphology in any of the three types of cultures (microalgal, bacterial, or co-culture, Figure 2).

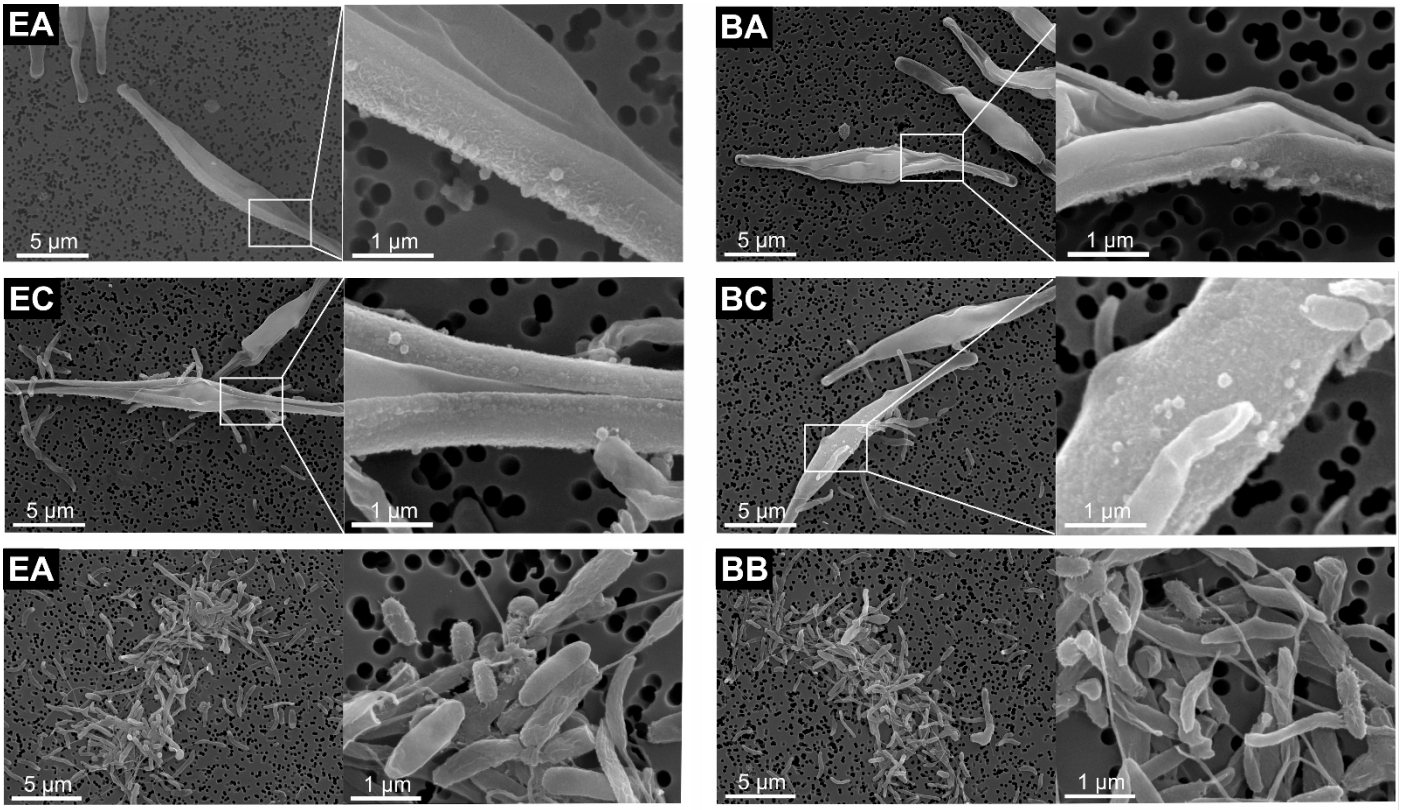

Figure 2. Scanning electron microscopy images of Experimental (left side) and Blank (right side) cultures of Axenic microalgae (EA, BA, respectively), Co-culture (EC, BC, respectively) and Bacteria (EB, BB, respectively).

Isolates of SCPs from the microalgal and co-cultures were rich in globular particles with a distinctly rough surface (Figure 3, panel E and Figures A1 and A2). Such structures were observed in some regions of microalgal cells with a rough, nanostructured epitheca (e.g. Figure 2: EA) in all cultures containing microalgae (EA, BA, EC, and BC). Cryo-TEM microscopy of an isolate from an axenic microalgae culture showed two types of SCPs: electron-dense clusters and membrane-enclosed EVs (Figure 3, panel F, black and white arrowheads, respectively). The membrane of EVs was surrounded by radially oriented fibres, forming approximately 20 nm thick corona (Figure 3, panel F, Cryo-TEM). In the isolates samples from the bacterial cultures, we observed singular SCPs and buds having a smooth globular shape (Figure 3, panels A - D).

Preprints (www.preprints.org) | NOT PEER-REVIEWED | Posted: 17 June 2022 doi:10.20944/preprints202206.0244.v1

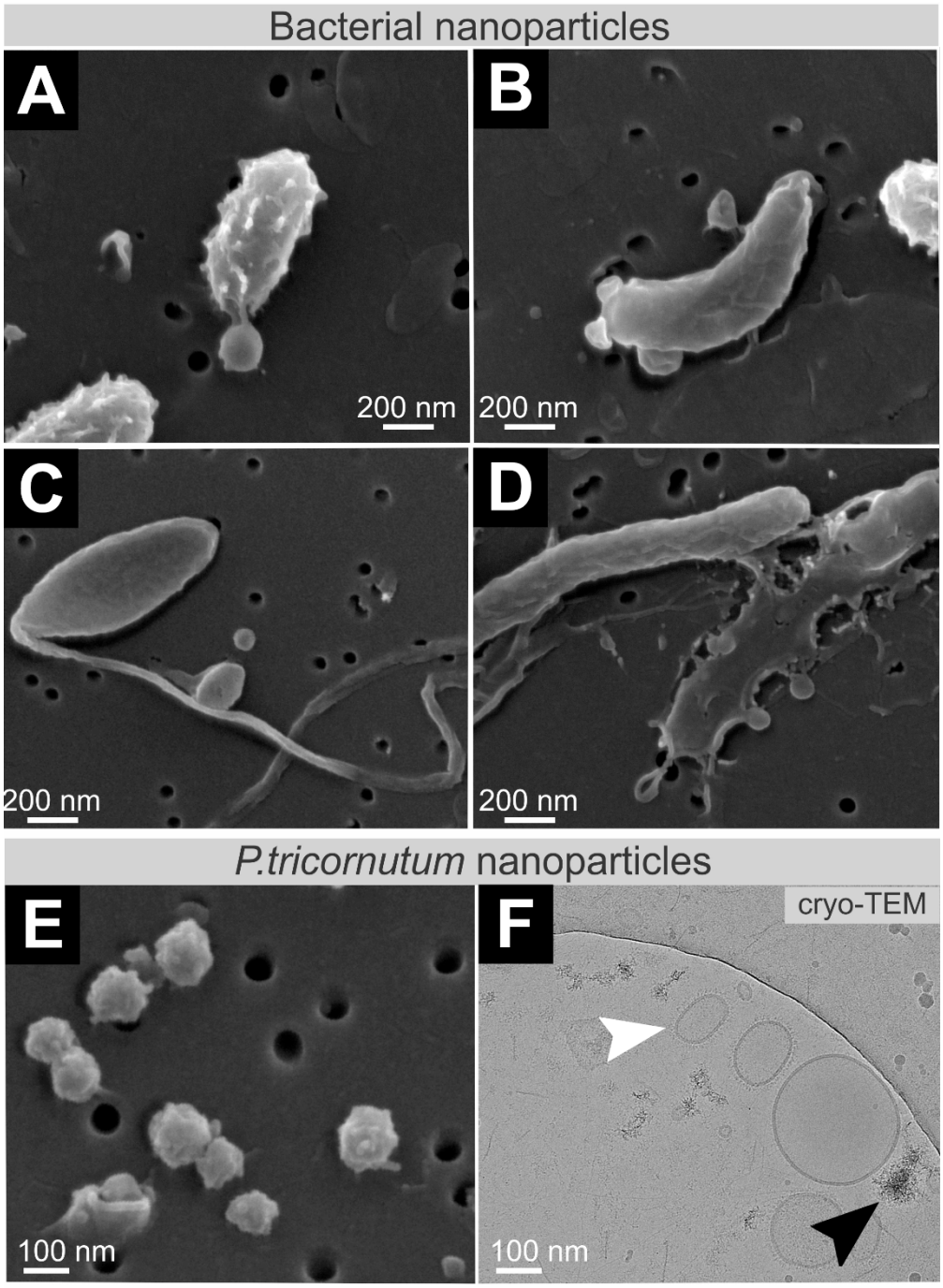

Figure 3. Electron microscopy imaging of osmium-fixed samples of bacterial (A-D) and *P. tricornutum* SCPs (E) and cryo-TEM image of *P. tricornutum* SCPs (F). The white arrowhead points to an EV, and the black arrowhead points to an electron-dense cluster.

The protein profile obtained by SDS-PAGE for EA and BA showed visible bands in the first two fractions, corresponding to microalgae, while the other three fractions had no visible bands (Figure 4: EA, BA). Bands corresponding to bacterial cultures were visible in the first four fractions of each series and only slightly in the SCP fraction (Figure 4: EB, BB). In the co-cultures, we could observe bands characteristic of microalgae in the first fractions. The following three fractions had bands characteristic of bacteria. Only slightly visible bands were present in the final SCP fractions (Figure 4: EC, BC). Extraction of proteins from the microalgal cells was less efficient in the case of the co-culture samples, resulting in less visible bands. We observed no effects of BPs and co-cultures on the protein

 doi:10.20944/preprints202206.0244.v1

profiles (bands obtained by SDS-PAGE) in any of the three cultures: microalgal, bacterial, or co-culture (Figure 4). The amount of proteins in the isolates was too low to allow comparison between samples, as bands were not visible after staining.

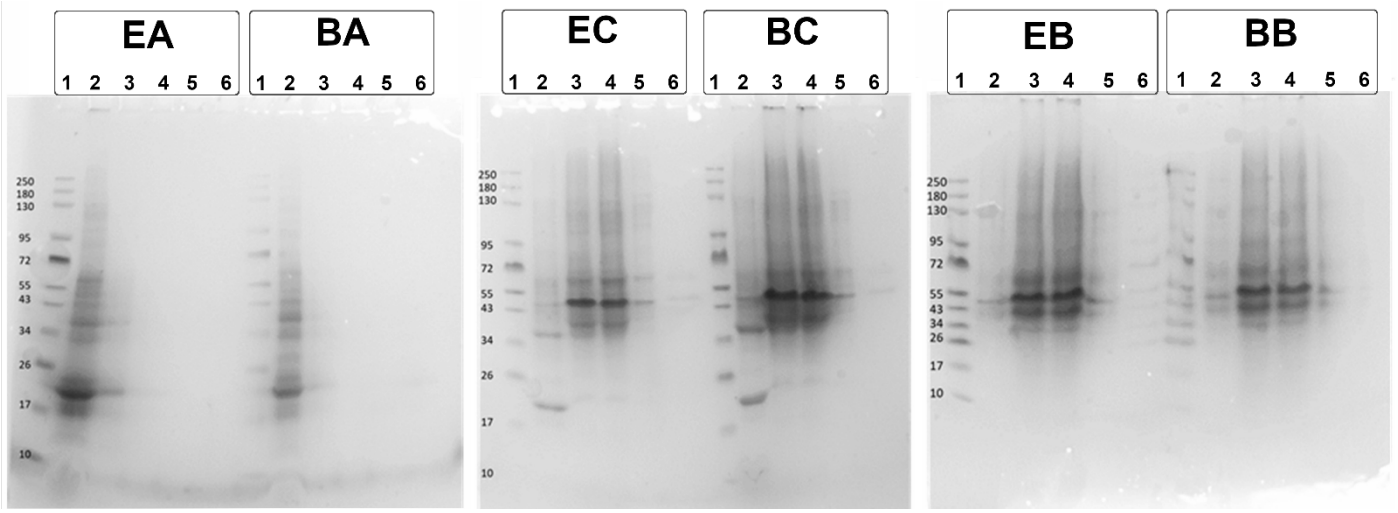

Figure 4. Protein profiles of axenic microalgae (EA, BA), co-cultures (EC, BC) and bacterial cultures (EB, BB). Numbers denote the content of wells: 1 - commercial size marker, 2-6 - different pellets derived by differential centrifugation: 2 - 660 g for 20 min, 3 - 2640 g for 22 min, 4 - 4000 g for 60 min, 5 - 4000 g for 90 min and 6 - 118 000 g for 70 min (SCP isolate).

2.3. Bisphenol residue mass balance and removal

Concentrations of BPs in either the abiotic light (ABL) or abiotic dark (ABD) controls show no appreciable decrease between 72 h and 168 h (Figure A4). Likewise, no significant differences were observed between the abiotic light (ABL) and abiotic dark (ABD) series, indicating that no photodegradation took place (Figure A4). Their higher hydrophobicity can also explain the lower concentrations of BPFL–BPPH than their nominal starting concentrations (C0 = 1000 ng/L) as a result of adsorption (49%) to the glass walls of the vessel [32]. The blank controls (BA, BC and BB) indicated no contamination with BPs, except for BPA, which reached 100 ng L^{-1} in one BA microalgae culture (not shown). However, determining BPA accurately at low levels can be problematic due to background contamination [33].

After 168 h, the proportion of BPs residues in biomass was highest for the more hydrophobic compounds (log P 5.99 – 7.34) BPFL, BPBP, BPM, BPP, and BPPH and ranged from 10 ± 4% (BPFL in axenic microalgae) to 30 ± 4% (BPPH in bacteria, Figure 5). Other more polar BPs' (BPS – BPAP, log P 2.32 – 5.18) were predominantly found in the aqueous phase (> 60%, Figure 5). The proportion of BPs in the aqueous phase ranged from <LOQ (BPC2 in axenic microalgae and co-culture) to 81 ± 5% (BPAF in axenic microalgae). Total removal ranged from 17 ± 5% (BPAF in axenic microalgae) to > 99% (BPC2 in axenic microalgae and co-culture). Removals between the cultures most notably differed for BPC2, BPC and BP26DM.

Preprints (www.preprints.org) | NOT PEER-REVIEWED | Posted: 17 June 2022 doi:10.20944/preprints202206.0244.v1

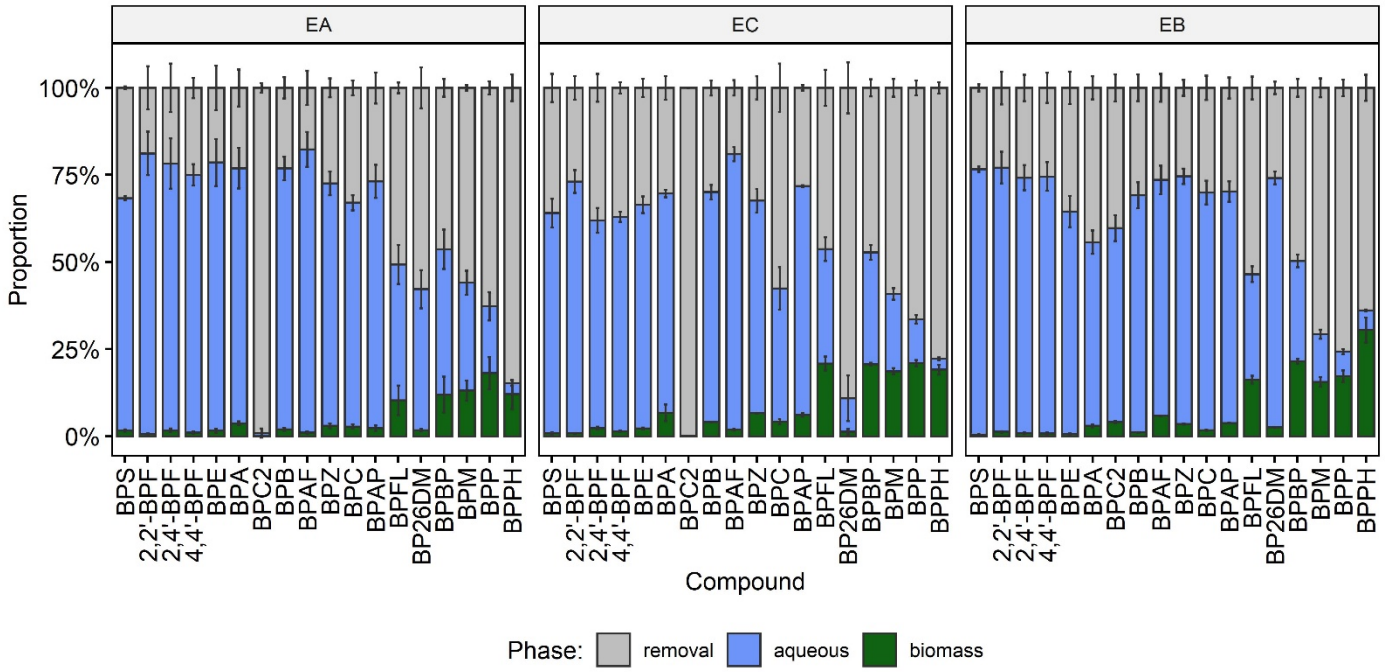

Figure 5. Proportion of BPs in microalgal culture, co-culture of microalgae and bacteria and culture of bacteria 168 h after addition of BPs to the medium. The proportions of the aqueous phase, biomass phase and calculated removal are shown with mean ± standard deviation. Compounds are arranged from lowest (BPS, log P = 2.3) to highest (BPPH, log P = 7.3) log P value.

Biotic removal (total removal - ABL, Figure 6) ranged from 0% (BP26DM, BPPH, BPFL, and BPAF) to 71 ± 0.1% (BPC2 in co-culture). Statistically significant differences ($p \leq 0.05$) between the three cultures were found for BPS, BPA, BPC2, BPC, BP26DM, BPM, BPP and BPPH. The last compound was the only one in which the axenic microalgae culture was the most efficient at removal, and the differences in biotic removal between cultures were relatively small (Figure 6). In the case of BPS, BPC and BP26DM, the co-culture proved the most efficient; however, for BPS, the removal in all three cultures was lower than 20%. The highest removals were detected for BPC2 in the microalgal (71 ± 1%) and co-culture (71 ± 0.1%). The removal of BPA (22 ± 3%), BPM (28 ± 3%) and BPP (24 ± 2%) was higher in the bacterial culture than in the algal cultures.

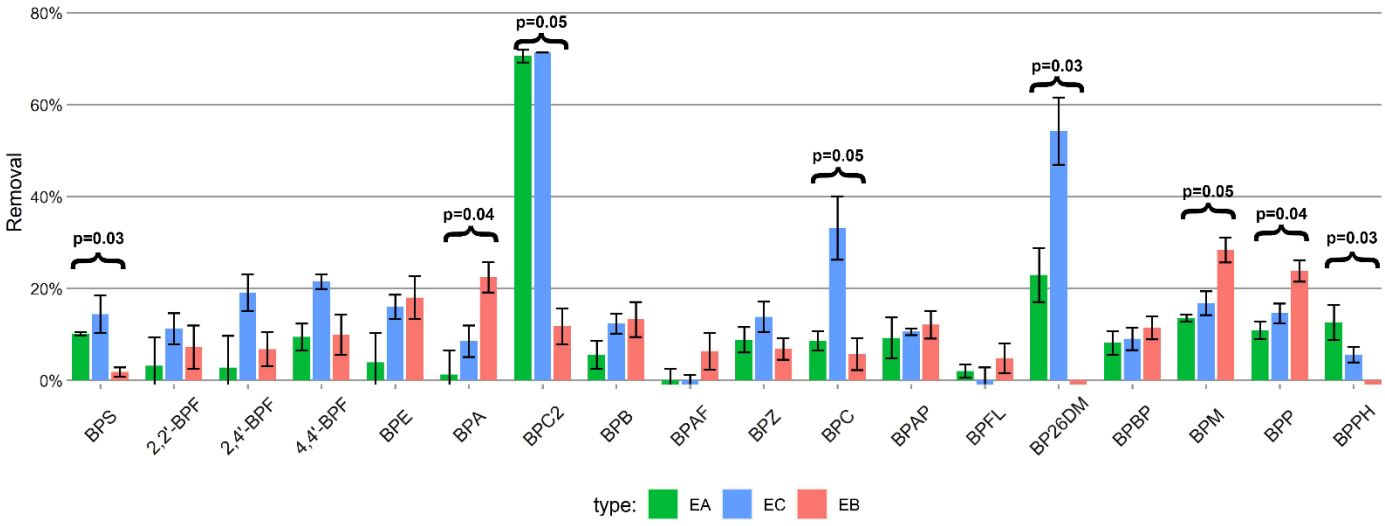

Preprints (www.preprints.org) | NOT PEER-REVIEWED | Posted: 17 June 2022 doi:10.20944/preprints202206.0244.v1

Figure 6. Biotic removal of BPs in microalgal culture, co-culture and culture of bacteria 168 h after addition of BPs to the medium. Compounds are arranged from lowest (BPS, log P = 2.3) to highest (BPPH, log P = 7.3) log P value.

Overall biotic removal (combined removal of all BPs) was, on average (white squares, Figure 7) highest in the co-culture (18 ± 18%), followed by the axenic culture (11 ± 15%) and lastly, the bacterial culture (10 ± 9%), however, differences between the three cultures series were not statistically significant ($p > 0.05$). The large SDs result from the broader range of biotic removal values of individual compounds.

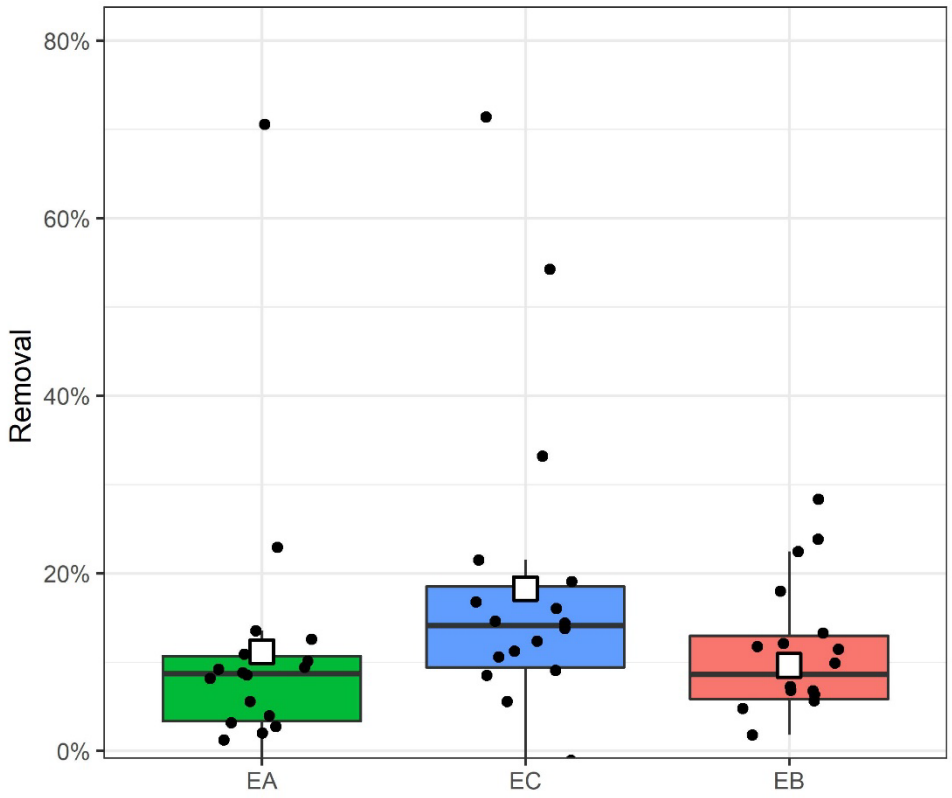

Figure 7. Overall biotic removal of all 18 BPs in microalgal culture, co-culture of microalgae and bacteria and culture of bacteria after 168 h. Boxplot explained: thick horizontal line is the median, box spans from the first to the third quartile, while whiskers span 1.5 interquartile range. Points representing the removal of individual compounds are also shown to observe their distribution easier.

3. Discussion

3.1. Culture growth

P. tricornutum grew exponentially throughout the experiment (Figure 1). The co-culture samples (Figure 1: EC and BC) reached a higher cell number density than the axenic ones (Figure 1: EA and BA), while the concentration of bacteria in both the co-culture and bacterial cultures reached the plateau phase of growth and declined towards the end of the experiment (Figure 1: EC, BC and EB, BB). Also, the bacterial growth rate and the maximum cell number density were lower in the co-culture (Figure 1: EC and BC) compared to the bacterial cultures (Figure 1: EB, BB). The organic nutrients supplied with the LB can explain these growth curves and cell concentration limits. In the co-cultures and bacterial cultures, organic residues from the bacterial inoculum (0.25 % working V) and an additional 1 % working V of LB broth were added. This finding means that approximately 4-times more nutrients were available from the LB supplementation in the bacterial cultures (EB, BB) compared to the co-culture samples (EC, BC). This is proportional to

 doi:10.20944/preprints202206.0244.v1

the maximum bacteria concentration reached in these two sample types (3.6 ± 0.7 x 10^6 mL^{-1} and 2.8 ± 0.2 x 10^6 mL^{-1}, in EC and BC, respectively, and 10.3 ± 0.4 x 10^6 mL^{-1} and 10.6 ± 1.1 x 10^6 mL^{-1}, in EB and BB, respectively, Figure 1). *P. tricornutum* is known to have antimicrobial activity against various bacteria [34–36]. The higher microalgal cell number densities in the co-culture samples (Figure 1: EC, BC) are likely a consequence of the positive effect of bacteria on microalgal growth, as observed in previous studies [37–39]. At the same time, microalgal and bacterial cells could be competing for nutrients from the small addition of a partially depleted LB medium during inoculation. No differences in growth rates (Figure 1) or cell morphology (Figure 2) were observed in cultures treated with BPs compared to the blank controls, suggesting that the concentrations of BPs used in the experiment were subtoxic to all microorganisms considered in this study.

3.2. Cell morphology, protein profile and nanoparticle characterization

The SEM imaging (Figure 2) and SDS-PAGE of the bacterial samples (Figure 4: EC, BC, EB, BB) showed no noticeable difference or shift in the microbial community due to the presence of *P. tricornutum* (Figure 2). Also, no zone of inhibition was observed between the microalgal and bacterial colonies on the solid media, indicating that *P. tricornutum* did not significantly affect bacterial growth in the cultures (Figure A3).

SEM revealed roughly spherical nanoparticles, 50-300 nm in size, were found in the isolates from all cultures containing *P. tricornutum* and homogenously sized (approx. 100nm) SCPs with a characteristically rough surface. Cryo-TEM revealed particles ranging in size from tens to hundreds of nanometers enclosed by a membrane and a fibrillar corona and recognized as *P. tricornutum* EVs (Figure 3, panel F, white arrowhead). However, cryo-TEM also revealed other types of SCPs, such as electron-dense clusters (Figure 3, panel F, black arrowhead). Therefore, it is not decisive what is the predominant type of SCPs in the culture and isolates. It was previously reported that the production of EVs in cell lines could be increased upon different types of stress, e.g. hypoxic stress [40], oxidative stress [41], nutrient stress [42] and others. However, EV production increased with the addition of BPs (Figure 2).

The number of proteins recovered in the isolates was too low to compare protein profiles. The residual bacteria hampered the observation of SCPs in isolates from the co- and bacterial cultures. Filtration of the isolates was not possible due to the small amount of sample (70 μL).

3.3. Bisphenol residue mass balance and removal

Residues of BPs followed a similar trend as seen in previous studies on BPs removal by microalgae [29], meaning that more residues of lipophilic (log P ≥ 6) compounds remained in the biomass phase while hydrophilic compounds (log P < 6) prevailed in the aqueous phase (Figure 5). Removal of BPS, BPC2, BPC, BP26DM and BPPH was higher in cultures with microalgal cells, while BPA, BPM and BPP removals were significantly higher in the bacterial cultures. However, BPM, BPP, and BPPH were mainly depleted in the abiotic controls. The co-culture was more efficient at removing BPs than both the axenic microalgae and bacterial cultures only in the case of BPC and BP26DM. This finding refutes our hypothesis that co-cultures are more efficient at removing BPs than single cultures. Instead, different cultures were efficient in removing different BPs. Removal of BPC2 (in EA and EC) and BP26DM (in EC) were the only cases where biotic removal was higher than 50%, constituting an appreciable fraction (Figure 6). However, in most cases, after 168 hours, biotic removal was lower than 30%. Contrary to expectations, our results show that the co-culture was not uniformly more efficient at BPs removal than the axenic microalgae or bacterial series.

Compared to *C. vulgaris*, which, except for BPC2, reached more than 50% biotic removal after 144 hours for 2,4'-BPF, 4,4'-BPF, BPC, BP26DM, and BPM [29], *P. tricornutum* was generally less efficient at BPs removal. Comparatively, a mixed culture of diverse

 doi:10.20944/preprints202206.0244.v1

microalgae and bacteria from a high-rate algal pond (HRAP) grown in wastewater performed much more efficiently, reaching an average biotic removal of 56% for 16 BPs [40], while *P. tricornutum* reached 11%, 19% and 10% on average in the cases of axenic microalgae, co-culture and bacterial cultures, respectively. However, the total removal efficiency of BPC2 was very similar in the axenic microalgae and co-culture in this study and the mixed culture from HRAP (88% ± 3%) [43]. While not as applicable for removal of CEC as *C. vulgaris*, further study of *P. tricornutum* is important for improving our understanding of SCPs and their role in intercellular communication.

Microalgae-based technologies that rely on microalgae communities and aerobic heterotrophic microorganisms (primarily bacteria) are promising alternatives to conventional biological wastewater treatment. Although many resources are exploited linearly (extract – use – disposal), the reuse of resources by recycling wastewater is in line with circular economy principles. One of the main advantages of utilizing microalgae-based wastewater treatment is nutrient- and energy-rich microalgal biomass production and production of reclaimed water. Notably, the valorization of biomass and reclaimed wastewater is in line with the principles of the EU's Circular Economy Action Plan [44]. It has been shown that microalgae-based wastewater treatment technologies may exhibit CEC removal efficiency comparable or superior to conventional biological systems [45,46].

Understanding microalgal-bacterial interactions are crucial for effective microalgae-based wastewater treatment, production of biomass and value-added products. Mutualistic interactions include the exchange of macronutrients, where bacteria benefit from fixed carbon from the microalgae, while bacteria may fix nitrogen in exchange [47]. Furthermore, micronutrient exchange may also occur, notably in the form of vitamin B_{12} or B_1 excretion by bacteria [47]. Signal transduction is another form of microalgal-bacterial interactions, where, e.g. bacterial secretions may induce morphogenesis in microalgae, microalgal secretions inhibit bacterial quorum sensing, or microalgae may inhibit the growth of bacteria and vice-versa [48]. Lastly, evidence in the chloroplast genome of diatoms and dinoflagellates and diatom ornithine-urea cycle genes point to horizontal gene transfer between microalgae and bacteria as another type of interaction that shaped such partnerships through evolutionary processes [48]. The study of microalgal–bacterial interactions is also of significance to understanding the underlying mechanisms of ecology (mutualistic or host-pathogen interactions, spreading of resistance, disease) and presents a significant applicative potential for biotechnology and other industries [49].

4. Materials and Methods

4.1. Cultures and medium composition

An axenic culture of the diatom *Phaeodactylum tricornutum* (CCAP 1052/1A, Culture Collection of Microalgae & Protozoa, Oban, Scotland) was chosen as the model organism. Additionally, two bacterial samples, one with prevailing Gram-positive and one with prevailing Gram-negative unidentified bacilli, were isolated from other in-house marine microalgal cultures for inclusion in the experiment. Cultures were grown in 300 ml Erlenmeyer flasks on an orbital shaker (Vibromix 40, Tehtnica, Slovenia) at 130 RPM. Irradiance was provided with Osram Fluora (Germany) fluorescent lights, resulting in approximately 41 ± 6 μmol m^2 s^{-1} of photosynthetically active radiation, with a photoperiod of 16:8 (light:dark).

Artificial marine water (MW) was prepared by dissolving 22 g/L of an artificial sea salt mix (Reef Crystals - Aquarium Systems, France) in distilled water. Guillard's (F/2) marine water enrichment solution (ref. nr. G0154, Sigma Aldrich, USA), and LB broth (ref. L3022, Sigma Aldrich, USA), were added to support microalgal and bacterial growth, respectively. In addition, MW-F/2 was prepared by adding 20 mL of enrichment solution per 1 L of MW. MW-LB was prepared by adding 20 g of LB per 1 L of MW. Solid MW-LB medium was prepared by adding 1% agar to MW-LB. All media were filtered through a

Preprints (www.preprints.org) | NOT PEER-REVIEWED | Posted: 17 June 2022 doi:10.20944/preprints202206.0244.v1

0.2-micron cellulose filter (ref. 11107-47-CAN, Sartorius Stedim Biotech GmbH, Germany) and autoclaved before use.

The microalgal cultures were inoculated into the inorganic medium of Guillard's f/2-enriched seawater (MW-f/2). Given that the medium was autoclaved, the concentration of biotin, thiamine and vitamin B_{12} was likely reduced before inoculation. Some LB broth (0.5% culture volume) was added to the co-cultures and bacterial cultures with the bacterial inoculum (already depleted in nutrients during the preculture). The medium for the bacterial cultures was additionally supplemented with 1% LB broth to ensure some bacterial growth. No additional LB broth was added to the co-cultures since the microalgae would provide organic support for bacterial growth. BPs were spiked into the experimental and abiotic control series by spiking 40 µL of a MeOH solution containing 5 mg/mL of each of the 18 BPs, resulting in a nominal concentration of 1 µg/L of each compound (Table 1). Individual compounds are identified in Table A1.

For bacterial inoculum, several colonies of bacteria were transferred from solid (1% MW-LB agar) to 2 mL of liquid MW-LB medium (20g/L) and allowed to grow for three days at room temperature on a rotational shaker (HulaMixer, Termofisher Scientific, USA) at 10 rpm. Two precultures were prepared – one with a prevailing unidentified gram-negative bacillus (isolated from a *Rhodella sp*. culture) and one with a prevailing gram-positive bacillus (isolated from *Tetraselmis chuii* culture). Before the experiment, both precultures were mixed before inoculation. In the experiment, the medium for bacterial cultures was supplemented with 1% MW-LB to provide a necessary amount of nutrients, predicted to be comparable to that provided by the microalgae in the co-culture. Cultures for the experiment were prepared as presented in Table 1. The experiment lasted for 168 h, and samples were taken for measurements of cell concentration of microalgae and bacteria (0 h, 72 h and 168 h), BPs concentration (72 h and 168 h) and EV isolation (168 h). To confirm the absence of bacteria (contamination) in axenic microalgal and abiotic cultures, they were inoculated on MW-LB agar plates at the end of the experiment and incubated at room temperature for 14 days.

Table 1. Preparation of series used in the experiment.

	Series	r*	f/2 [mL]	LB [mL]	microalgae inoculum [mL]	bacterial inoculum [mL]	bisphenol standard [µL]	blank MeOH [µL]	ill**
control series	abiotic dark (ABD)	3	200	0	0	0	40	0	NO
	abiotic light (ABL)	3	200	0	0	0	40	0	YES
	blank axenic microalgae (BA)	3	150	0	50	0	0	40	YES
	blank co-culture (BC)	3	149.5	0	50	0.5	0	40	YES
	blank bacteria (BB)	3	197.5	2	0	0.5	0	40	YES
experimental series	axenic microalgae (EA)	3	150	0	50	0	40	0	YES
	co-culture (EC)	3	149.5	0	50	0.5	40	0	YES
	bacteria (EB)	3	197.5	2	0	0.5	40	0	YES

* - replicates of the same series.
** - illumination with fluorescent tubes.

4.2. Cell concentration

The cell concentration in the culture samples was determined using a MACSQuant Analyzer flow cytometer (Miltenyi Biotec, Germany) and the related software. The following instrument settings were employed: FSC: 458 V; SSC: 467 V with a trigger was set to 1.48, B3: 300V; R1: 360 V. Non-fluorescent particles (NFP), corresponding to bacteria, cell debris and SCPs, were detected from the forward (FSC) and side scatter parameter

Preprints (www.preprints.org) | NOT PEER-REVIEWED | Posted: 17 June 2022 doi:10.20944/preprints202206.0244.v1

(SSC), as they are not autofluorescent. The microalgal cells were identified based on chlorophyll auto-fluorescence (AFP), detecting red emission (channels B3: 488nm/655-730 nm, and R1: 635 nm/655-730 nm). Both AFP and NFP were quantified in all experimental and blank control series to check for possible contamination by microalgae or bacteria. Examples of AFP and NFP flow cytometer diagrams are shown in Figure 8.

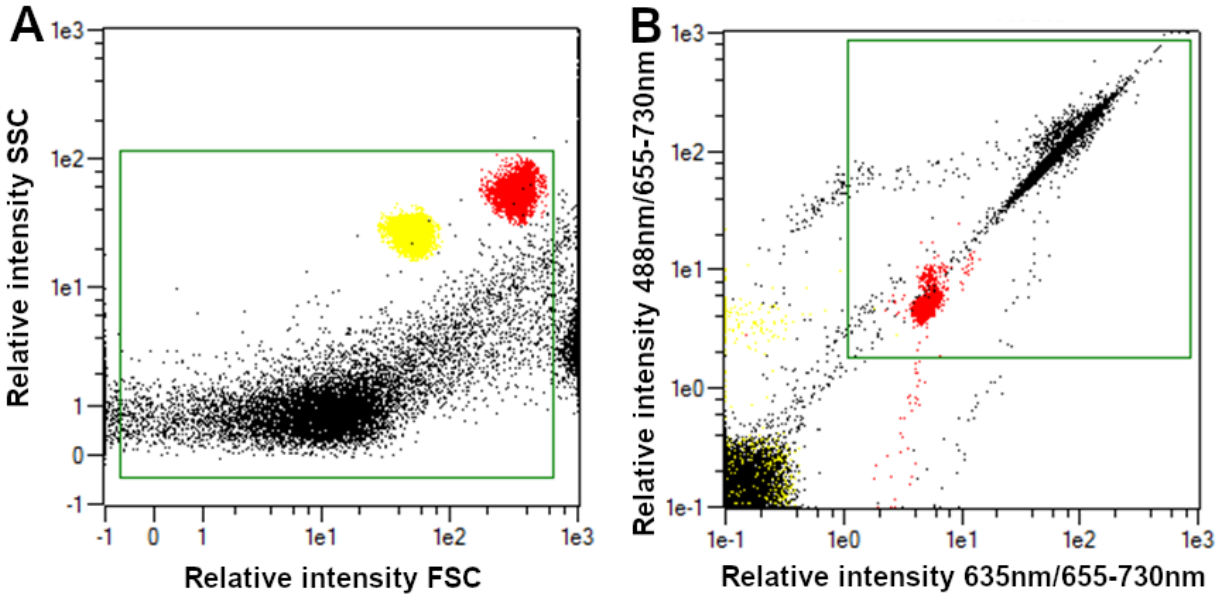

Figure 8. Flow cytometer plots of (A) NFP, attributed mainly to bacteria and SCPs; (B) AFP, attributed to microalgal cells. Clusters of fluorescent calibration beads are overlaid for comparison: 2 µm beads (left, yellow) and 3 µm beads (right, red). Yellow beads in B are clustered in the bottom left, with a negligible amount above that. Gates for selecting points for quantification of NFPs and AFPs (green squares) are also shown.

4.3. SCP isolation

SCPs were isolated by differential centrifugation. Cells and larger cell debris were cleared from the culture media in four centrifugation steps performed in a centrifuge Centric 400R (Domel, Železniki, Slovenia), using sterile polypropylene 15 mL conical centrifuge tubes 1: 660g, 20 min, 4°C; 2: 2640g 22 min, 4°C; 3: 4000g 60 min, 4°C; 4: 4000g, 90 min, 4°C. Finally, the nanoparticles remaining in the supernatant were pelleted by centrifugation at 118 000 g, 70 min, 4°C (Ultracentrifuge Beckman L8-70M, rotor SW 55Ti, using thin open-top polypropylene tubes ref. nr. 326819 Beckman Coulter, Inc., USA). The supernatant was removed, and the pellets were suspended in the remaining residual supernatant.

4.4. SEM imaging

Samples of cultures and SCP isolates were applied on polycarbonate filter membrane (0.2-micron Isopore™, ref. GTTP01300, Merk Millipore Ltd, Ireland were used for culture samples, and 0.05-micron, ref. PCT00513100, Sterlitech, the USA for NPs samples). Samples were then incubated for two hours in 2 % OsO_4. The unbound osmium was removed by three steps of washing in distilled water 10-min incubation was performed in each step before changing the solution. Then, samples were dehydrated in a graded series of ethanol (30 %, 50 %, 70 %, 80 %, 90 %, absolute), treated with hexamethyldisilazane (30 %, 50 % mixtures with absolute ethanol, followed by pure hexamethyldisilazane), and air-dried. The samples were Au/Pd coated (PECS Gatan 682) and examined using a JSM-6500F Field Emission Scanning Electron Microscope (JEOL Ltd., Tokyo, Japan).

4.5. Cryo-TEM imaging

 doi:10.20944/preprints202206.0244.v1

Samples of SCPs were prepared using Vitrobot Mark IV (Thermo Fisher Scientific, Waltham, MA, US). Quantifoil® R 2/2, 200 mesh holey carbon grids (Quantifoil Micro Tools GmbH, Großlöbichau, Germany) were glow discharged for 60 s at 20 mA and positive polarity in the air (GloQube® Plus, Quorum, Laughton, UK). Conditions were set at 4 °C, 100% relative humidity, blot time: 5 s, and blot force: 4. 2 µL of the sample with SCPs in suspension was applied to the grid, blotted, and vitrified in liquid ethane. Samples were visualized under cryogenic conditions using a 200 kV microscope Glacios with Falcon 3EC detector (Thermo Fisher Scientific, Waltham, MA, US). The total electron dose was 30 e/A^2.

4.6. Protein gel electrophoresis

Sodium dodecyl sulphate polyacrylamide gel electrophoresis (SDS-PAGE) in reducing conditions was performed using a True-Page precast gel 4-20 % (ref. PCG2004, Sigma Aldrich, Germany) and the suitable corresponding buffers. Before being loaded on the gel, 20 uL of the samples were mixed with 7 uL of 8 M urea, 3 uL of 10× dithiothreitol reducer and 10 uL of 4× loading buffer and heated at 95 °C for 5 minutes. Gels were resolved using constant current mode (set to 100 mA), and the coomassie blue-stained gels were imaged by Alliance Q9 Advanced Imager (Cleaver Scientific, UK).

4.7. Bisphenol quantification

Sample preparation was conducted as described in Škufca et al. (2021) [47]. Briefly, samples were centrifuged at 6000 RCF for 20 min to separate the aqueous and biomass phase. A standard internal mixture (final concentration in the sample: 500 ng L^{-1} of BPAd$_{16}$, ^{13}C$_{12}$-BPF, ^{13}C$_{12}$-BPS and ^{13}C$_{12}$-BPB each, 25 µL of 1 µg mL^{-1} solution) was also added, and the sample was filtered. The samples were then acidified and loaded onto MCX Prime (Waters, USA) solid-phase extraction (SPE) cartridges. The biomass phase was lyophilized and extracted with ACN/MeOH (80:20). Extracts were solvent exchanged to 4.5 mL EtAc/Hex (25:75) and purified with Bond Elut Carbon/PSA (Agilent, USA) SPE cartridges.

Bisphenols were analyzed using gas chromatography (GC, model 7890B, Agilent, USA) with tandem mass spectrometry (MS/MS, model 7000, Agilent, USA). Separation was achieved using a DB-5 MS capillary column (30 m × 0.25 mm × 0.25 µm; Agilent, USA) with helium as the carrier gas. Samples were injected in splitless mode at 270 °C. The compounds were ionized in electron impact (EI) mode at 70 eV and detected using multiple reaction monitoring modes (MRM). The total runtime was 24 min.

4.8. Data analysis

Physico-chemical properties of BPs (log P) were predicted based on compound structure, using the Marvin Suite [51]. Data analysis and visualization were performed using the R programming language [52] in the R Studio environment [53]. The software packages "tidyverse" [54], "xslx" [55] and "rstatix" [56] were used to analyze the data. The Kruskal-Wallis one-way analysis of variance was used to determine significant differences between series. BPs removal was calculated according to measured BPs' mass in each phase (m_a - aqueous and m_b - biomass) at a given time according to the initial nominal spiked mass (m_0 being 200 ng, equal to a spiked concentration of 1000 ng L^{-1} per compound). Removal was calculated as total removal using the following equation:

$$Removal_T\ (\%) = \frac{(m_0 - (m_a + m_b))}{m_0}\ x\ 100\%$$

The biotic removal was calculated by subtracting the total removal in the abiotic light control (ABL) series from the total removal of the experimental series:

$$Removal_{BIO}\ (\%) = Removal_T - \text{Removal}_{ABL}$$

5. Conclusions

 doi:10.20944/preprints202206.0244.v1

We studied the cell growth, protein profiles, SEM and cryo-TEM images of SCPs, and compound removal of three culture types: axenic culture of P. tricornutum microalgae, bacterial culture and a co-culture of both. Our study found that the growth of microalgae in co-culture with bacteria was enhanced compared with axenic microalgae. Also, the protein profiles of the cultures remained independent of treatment, indicating that BPs did not affect protein expression, while protein content in SCP isolates was insufficient for comparison. Apart from differences in the number of SCP, no qualitative differences in nanoparticle isolates of the three cultures were observed regarding exposure to BPs using SEM. We observed differences in BP removal in eight of the BPs between the three cultures, and although it is not clear which mechanism influences removal efficiency in a given culture type, it indicates that the different cultures were variously effective for removing different BPs. Finally, continued study of intercellular communication in connection with small cellular particles is important in the future for both having a basic understanding of ecological interactions and improving the biotechnical applications of microalgae-bacterial cultures.

Supplementary Materials: The following supporting information can be downloaded at: www.mdpi.com/xxx/s1, Table S1: Raw data of BPs analysis.

Author Contributions: Conceptualization: David Škufca, Darja Božič, Ester Heath, Veronika Kralj-Iglič. Formal analysis: David Škufca, Darja Božič. Funding Acquisition: Veronika Kralj-Iglič, Tjaša Griessler Bulc, Ester Heath, Aleš Iglič. Investigation: David Škufca, Darja Božič, Matej Hočevar, Marko Jeran, Apolonija Bedina Zavec, Matic Kisovec, Tadeja Matos, Rok Tomazin. Resources: Veronika Kralj-Iglič, Tjaša Griessler Bulc, Ester Heath, Aleš Iglič, Matej Hočevar, Marjetka Podobnik. Supervision: Veronika Kralj-Iglič, Tjaša Griessler Bulc, Ester Heath. Visualization: David Škufca, Darja Božič, Matej Hočevar. Writing - original draft: David Škufca, Darja Božič. Writing - review & editing: Veronika Kralj-Iglič, Tjaša Griessler Bulc, Ester Heath, Marjetka Podobnik, Apolonija Bedina Zavec, Matic Kisovec.

Funding: This research was funded by the Slovenian Research Agency, namely Program Groups P3-0388, P2-0232, P2-0132 and Projects J3-3066, L3-2621.

Data Availability Statement: Data may be obtained by contacting authors.

Conflicts of Interest: The authors declare no conflict of interest.

Sample Availability: Samples for SEM imaging are available from the authors.

Appendix A

Table A1. Bisphenol compound abbreviations, IUPAC names and CAS identifiers.

Abbreviation	IUPAC name	CAS
BPA	4-[2-(4-hydroxyphenyl)propan-2-yl]phenol	80-05-7
2,2′-BPF	2-[(2-hydroxyphenyl)methyl]phenol	2467-02-9
2,4′-BPF	2-[(4-hydroxyphenyl)methyl]phenol	2467-03-0
4,4′-BPF	4-[(4-hydroxyphenyl)methyl]phenol	620-92-8
BP26DM	4-[2-(4-hydroxy-3,5-dimethylphenyl)propan-2-yl]-2,6-dimethylphenol	5613-46-7
BPAF	4-[1,1,1,3,3,3-Hexafluoro-2-(4-hydroxyphenyl)propan-2-yl]phenol	1478-61-1
BPAP	4-[1-(4-hydroxyphenyl)-1-phenylethyl]phenol	1571-75-1
BPB	4-[2-(4-hydroxyphenyl)butan-2-yl]phenol	77-40-7
BPBP	4-[(4-hydroxyphenyl)-diphenylmethyl]phenol	1844-01-5
BPC	4-[2-(4-hydroxy-3-methylphenyl)propan-2-yl]-2-methylphenol	79-97-0
BPC II	4-[2,2-dichloro-1-(4-hydroxyphenyl)ethenyl]phenol	14868-03-2
BPE	4-[1-(4-hydroxyphenyl)ethyl]phenol	2081-08-5
BPFL	4-[9-(4-hydroxyphenyl)fluoren-9-yl]phenol	3236-71-3
BPM	4-[2-[3-[2-(4-hydroxyphenyl)propan-2-yl]phenyl]propan-2-yl]phenol	13595-25-0

 doi:10.20944/preprints202206.0244.v1

BPP	4-[2-[4-[2-(4-hydroxyphenyl)propan-2-yl]phenyl]propan-2-yl]phenol	2167-51-3
BPPH	4-[2-(4-hydroxy-3-phenylphenyl)propan-2-yl]-2-phenylphenol	24038-68-4
BPS	4-(4-hydroxyphenyl)sulfonylphenol	80-09-1
BPZ	4-[1-(4-hydroxyphenyl)cyclohexyl]phenol	843-55-0

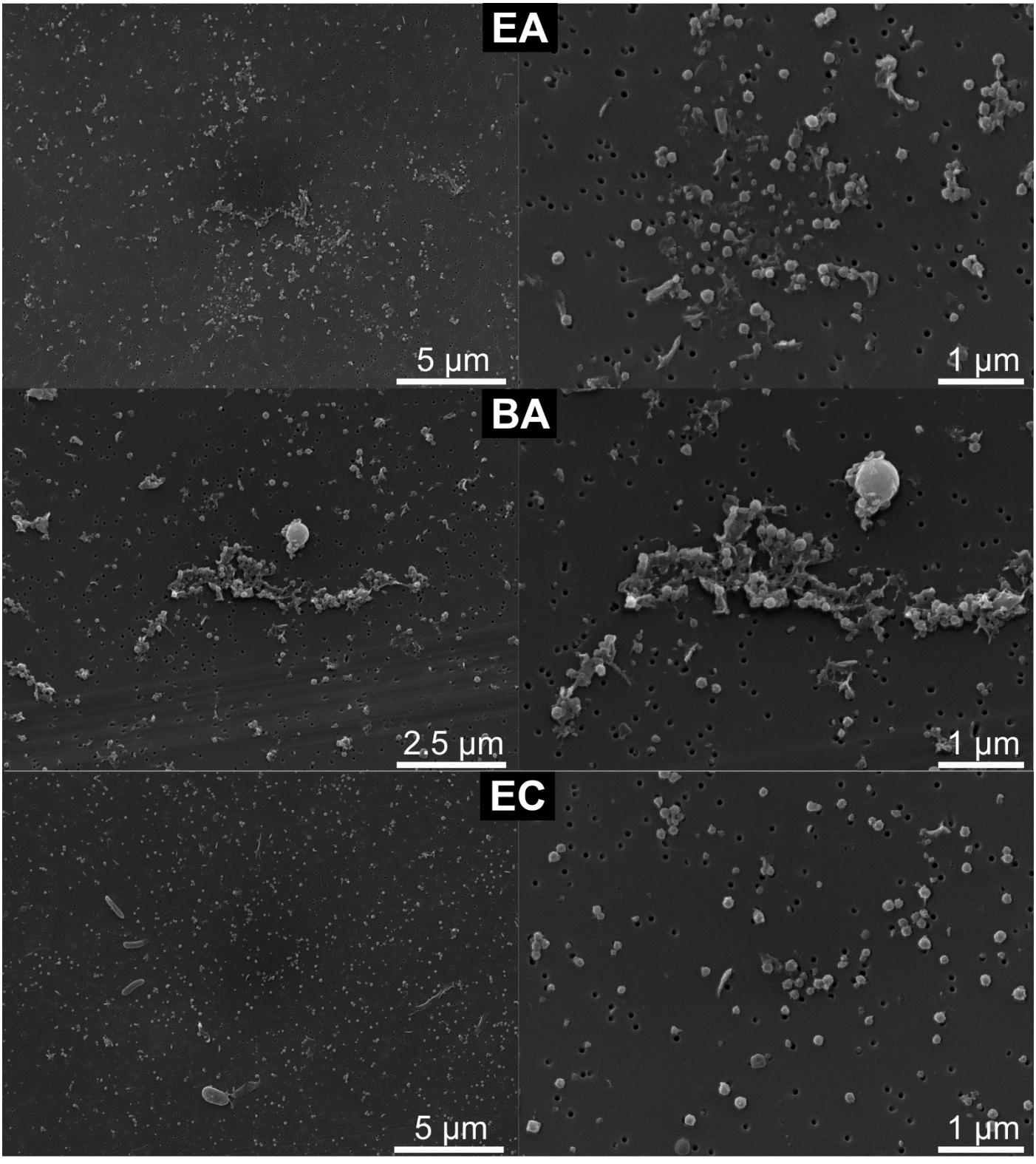

 doi:10.20944/preprints202206.0244.v1

Figure A1. Additional SEM images of SCP isolates from EA, BA, and EC cultures.

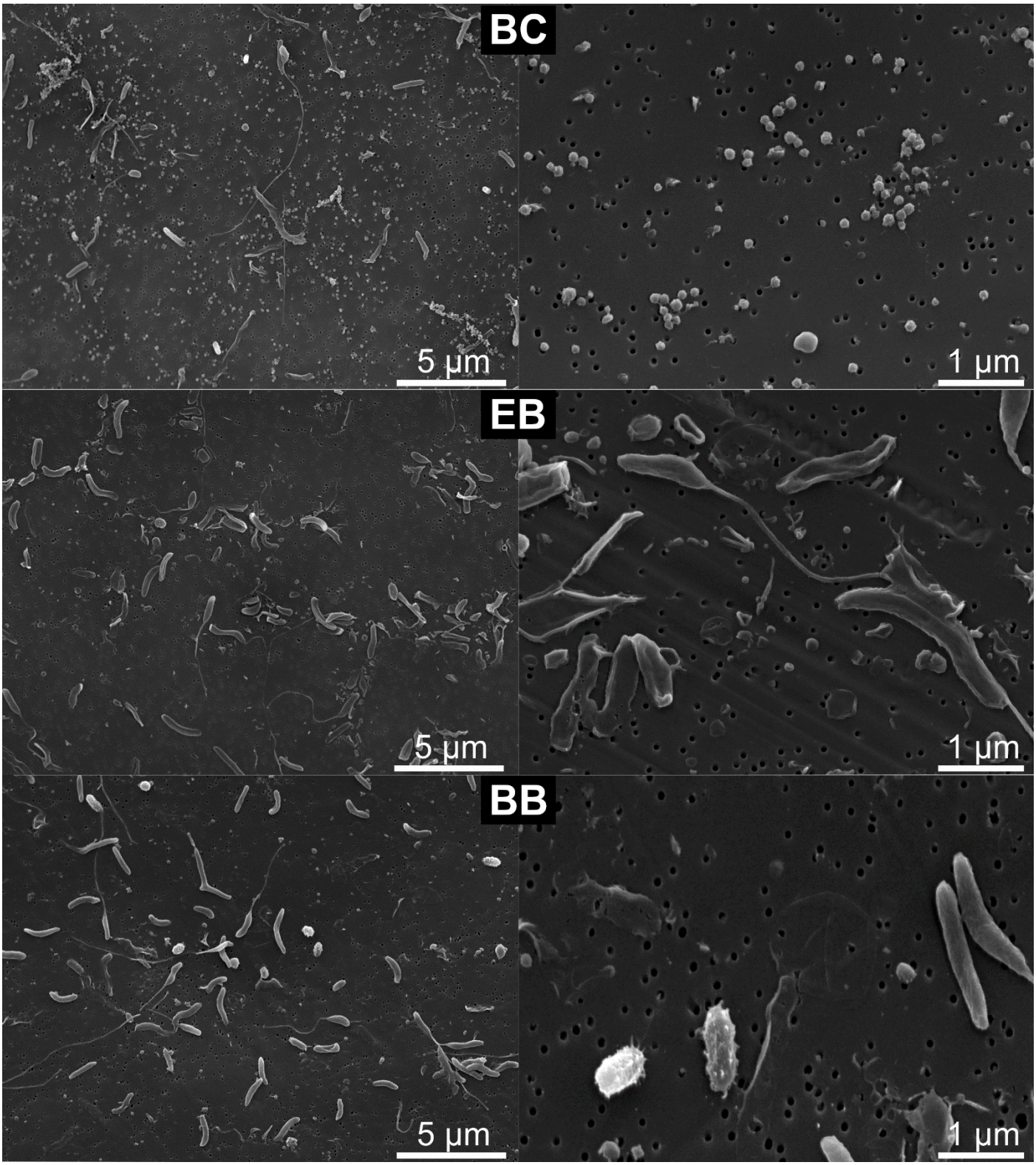

Figure A2. Additional SEM images of SCP isolates from cultures BC, EB and BB.

Preprints (www.preprints.org) | NOT PEER-REVIEWED | Posted: 17 June 2022 doi:10.20944/preprints202206.0244.v1

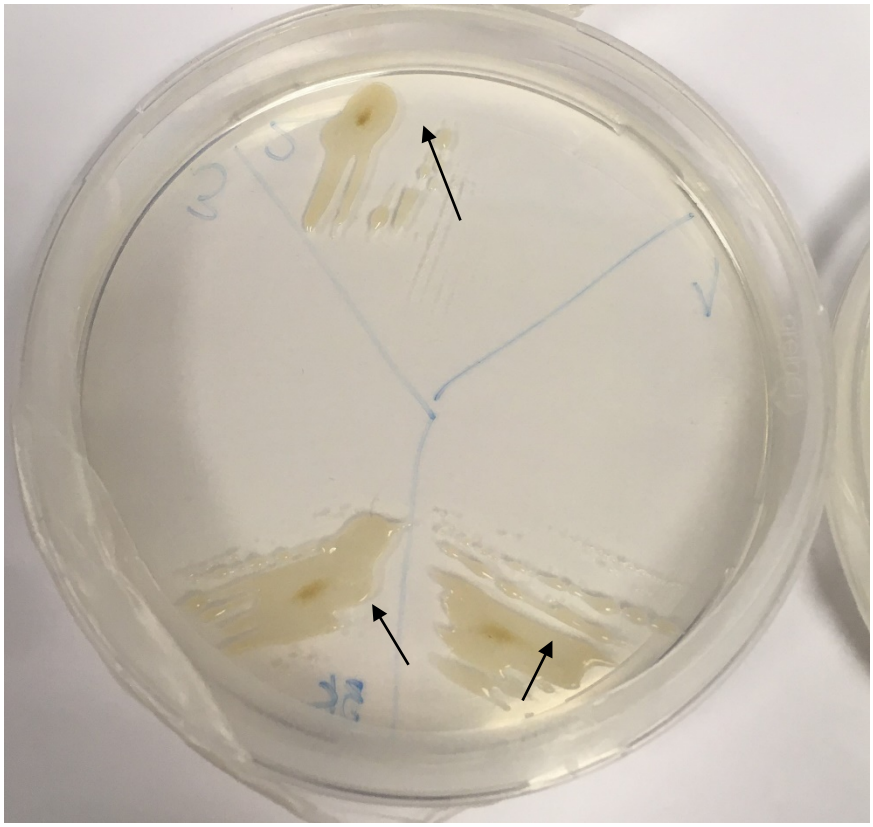

Figure A3. Co-culture sample grown on an agar plate, showing growth of bacteria, with microalgae *P. tricornutum* growth in the middle of bacterial growth (arrows).

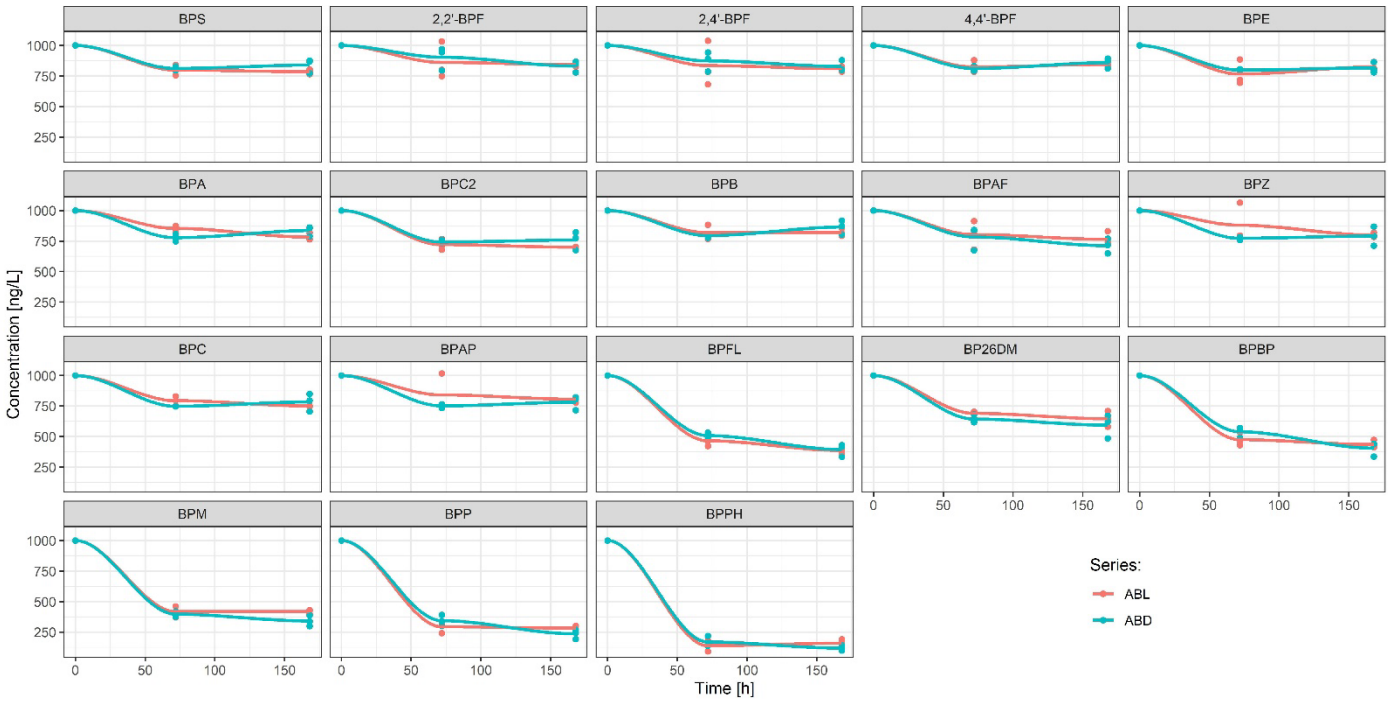

Figure A4. Abiotic control samples of 18 BPs in light (ABL) and dark (ABD) conditions. Compounds are arranged from lowest (BPS, log P = 2.3) to highest (BPPH, log P = 7.3) log P value.

References

1. Langergraber, G.; Castellar, J.A.C.; Andersen, T.R.; Andreucci, M.-B.; Baganz, G.F.M.; Buttiglieri, G.; Canet-Martí, A.; Carvalho, P.N.; Finger, D.C.; Griessler Bulc, T.; et al. Towards a cross-sectoral view of nature-based solutions for enabling circular cities. *Water* **2021**, *13*, 2352, doi:10.3390/w13172352.
2. Norvill, Z.N.; Shilton, A.; Guieysse, B. Emerging contaminant degradation and removal in algal wastewater treatment ponds: Identifying the research gaps. *J. Hazard. Mater.* **2016**, *313*, 291–309, doi:10.1016/j.jhazmat.2016.03.085.
3. Craggs, R.; Sutherland, D.; Campbell, H. Hectare-scale demonstration of high rate algal ponds for enhanced wastewater treatment and biofuel production. *J. Appl. Phycol.* **2012**, *24*, 329–337, doi:10.1007/s10811-012-9810-8.
4. Sutherland, D.L.; Park, J.; Heubeck, S.; Ralph, P.J.; Craggs, R.J. Size matters – Microalgae production and nutrient removal in wastewater treatment high rate algal ponds of three different sizes. *Algal Res.* **2020**, *45*, 101734, doi:10.1016/j.algal.2019.101734.
5. Brennan, L.; Owende, P. Biofuels from microalgae-A review of technologies for production, processing, and extractions of biofuels and co-products. *Renew. Sustain. Energy Rev.* **2010**, *14*, 557–577, doi:10.1016/j.rser.2009.10.009.
6. Park, J.B.K.; Craggs, R.J.; Shilton, A.N. Wastewater treatment high rate algal ponds for biofuel production. *Bioresour. Technol.* **2011**, *102*, 35–42, doi:10.1016/j.biortech.2010.06.158.
7. Rahman, M.A.; Aziz, M.A.; Al-khulaidi, R.A.; Sakib, N.; Islam, M. Biodiesel production from microalgae Spirulina maxima by two step process: Optimization of process variable. *J. Radiat. Res. Appl. Sci.* **2017**, *10*, 140–147, doi:10.1016/j.jrras.2017.02.004.
8. Rahman, A.; Putman, R.J.; Inan, K.; Sal, F.A.; Sathish, A.; Smith, T.; Nielsen, C.; Sims, R.C.; Miller, C.D. Polyhydroxybutyrate production using a wastewater microalgae based media. *Algal Res.* **2015**, *8*, 95–98, doi:10.1016/j.algal.2015.01.009.
9. Armingol, E.; Officer, A.; Harismendy, O.; Lewis, N.E. Deciphering cell–cell interactions and communication from gene expression. *Nat. Rev. Genet.* **2021**, *22*, 71–88, doi:10.1038/s41576-020-00292-x.
10. Combarnous, Y.; Nguyen, T.M.D. Cell Communications among microorganisms, plants, and animals: origin, evolution, and interplays. *Int. J. Mol. Sci.* **2020**, *21*, 8052, doi:10.3390/ijms21218052.
11. Jin, S.; Guerrero-Juarez, C.F.; Zhang, L.; Chang, I.; Ramos, R.; Kuan, C.-H.; Myung, P.; Plikus, M. V.; Nie, Q. Inference and analysis of cell-cell communication using CellChat. *Nat. Commun.* **2021**, *12*, 1088, doi:10.1038/s41467-021-21246-9.
12. Gill, S.; Catchpole, R.; Forterre, P. Extracellular membrane vesicles in the three domains of life and beyond. *FEMS Microbiol. Rev.* **2019**, *43*, 273–303, doi:10.1093/femsre/fuy042.
13. Aaronson, S. The synthesis of extracellular macromolecules and membranes by a population of the phytoflagellate Ochromonas danica. *Limnol. Oceanogr.* **1971**, *16*, 1–9, doi:10.4319/lo.1971.16.1.0001.
14. McLean, R.J.; Laurendi, C.J.; Brown, R.M. The Relationship of Gamone to the Mating Reaction in Chlamydomonas moewusii. *Proc. Natl. Acad. Sci.* **1974**, *71*, 2610–2613, doi:10.1073/pnas.71.7.2610.
15. Bozic, D.; Hocevar, M.; Jeran, M.; Kisovec, M.; Bedina Zavec, A.; Romolo, A.; Škufca, D.; Podobnik, M.; Kogej, K.; Iglič, A.; Touzet, N.; Manno, M.; Bongiovanni, A.; Kralj-Iglic, V. Ultrastructure and stability of cellular nanoparticles isolated from *Phaeodactylum tricornutum* and *Dunaliella tertiolecta* conditioned media. Sumbitted to *Open Research Europe*
16. Picciotto, S.; Barone, M.E.; Fierli, D.; Aranyos, A.; Adamo, G.; Božič, D.; Romancino, D.P.; Stanly, C.; Parkes, R.; Morsbach, S.; et al. Isolation of extracellular vesicles from microalgae: towards the production of sustainable and natural nanocarriers of bioactive compounds. *Biomater. Sci.* **2021**, *9*, 2917–2930, doi:10.1039/D0BM01696A.
17. Adamo, G.; Fierli, D.; Romancino, D.P.; Picciotto, S.; Barone, M.E.; Aranyos, A.; Božič, D.; Morsbach, S.; Raccosta, S.; Stanly, C.; et al. Nanoalgosomes: Introducing extracellular vesicles produced by microalgae. *J. Extracell. Vesicles* **2021**, *10*, doi:10.1002/jev2.12081.
18. Noguera-Oviedo, K.; Aga, D.S. Lessons learned from more than two decades of research on emerging contaminants in the environment. *J. Hazard. Mater.* **2016**, *316*, 242–251, doi:10.1016/j.jhazmat.2016.04.058.
19. Tolboom, S.N.; Carrillo-Nieves, D.; de Jesús Rostro-Alanis, M.; de la Cruz Quiroz, R.; Barceló, D.; Iqbal, H.M.N.; Parra-Saldivar, R. Algal-based removal strategies for hazardous contaminants from the environment – A review. *Sci. Total Environ.* **2019**, *665*, 358–366, doi:10.1016/j.scitotenv.2019.02.129.
20. Yadav, D.; Rangabhashiyam, S.; Verma, P.; Singh, P.; Devi, P.; Kumar, P.; Hussain, C.M.; Gaurav, G.K.; Kumar, K.S. Environmental and health impacts of contaminants of emerging concerns: Recent treatment challenges and approaches. *Chemosphere* **2021**, *272*, 129492, doi:10.1016/j.chemosphere.2020.129492.
21. Geens, T.; Goeyens, L.; Covaci, A. Are potential sources for human exposure to bisphenol-A overlooked? *Int. J. Hyg. Environ. Health* **2011**, *214*, 339–347, doi:10.1016/j.ijheh.2011.04.005.
22. Vehar, A.; Kovačič, A.; Hvala, N.; Škufca, D.; Levstek, M.; Stražar, M.; Žgajnar Gotvajn, A.; Heath, E. Fate of bisphenols during conventional wastewater treatment. *Proceedings of Socratic Lectures.* **2021**; 6: 57-62. https://doi.org/10.55295/PSL.2021.D.008.
23. Chen, D.; Kannan, K.; Tan, H.; Zheng, Z.; Feng, Y.-L.; Wu, Y.; Widelka, M. Bisphenol analogues other than BPA: environmental occurrence, human exposure, and toxicity—A review. *Environ. Sci. Technol.* **2016**, *50*, 5438–5453, doi:10.1021/acs.est.5b05387.
24. Muñoz, I.; López-Doval, J.C.; Ricart, M.; Villagrasa, M.; Brix, R.; Geiszinger, A.; Ginebreda, A.; Guasch, H.; de Alda, M.J.L.; Romaní, A.M.; et al. Bridging levels of pharmaceuticals in river water with biological community structure in the Llobregat river basin (northeast Spain). *Environ. Toxicol. Chem.* **2009**, *28*, 2706, doi:10.1897/08-486.1.
25. Sutherland, D.L.; Ralph, P.J. Microalgal bioremediation of emerging contaminants - Opportunities and challenges. *Water Res.* **2019**, *164*, 114921, doi:10.1016/j.watres.2019.114921.

26. Škufca, D.; Prosenc, F.; Kovačič, A.; Buttiglieri, G.; Heath, D.; Griessler Bulc, T.; Heath, E. Removal of contaminants of emerging concern in algal photobioreactors: from lab-scale to pilot-scale. *Proceedings of Socratic Lectures:* **2021**; 6: 207. https://www.zf.uni-lj.si/images/stories/datoteke/Zalozba/Sokratska_6.pdf
27. Maryjoseph, S.; Ketheesan, B. Microalgae based wastewater treatment for the removal of emerging contaminants: A review of challenges and opportunities. *Case Stud. Chem. Environ. Eng.* **2020**, *2*, 100046, doi:10.1016/j.cscee.2020.100046.
28. Liu, R.; Li, S.; Tu, Y.; Hao, X. Capabilities and mechanisms of microalgae on removing micropollutants from wastewater: A review. *J. Environ. Manage.* **2021**, *285*, 112149, doi:10.1016/j.jenvman.2021.112149.
29. Božič, D.; Hočevar, M.; Jeran, M.; Matos, T.; Tomazin, R.; Pocsfalvi, G.; Iglič, A.; Kralj-Iglič V. Scanning electron microscopy of microorganisms growing in co-cultures with microalgae. *Proceedings of Socratic Lectures.* **2021**; 6: 206. https://www.zf.uni-lj.si/images/stories/datoteke/Zalozba/Sokratska_6.pdf
30. Ji, X.; Jiang, M.; Zhang, J.; Jiang, X.; Zheng, Z. Bioresource Technology The interactions of algae-bacteria symbiotic system and its effects on nutrients removal from synthetic wastewater. *Bioresour. Technol.* **2018**, *247*, 44–50, doi:10.1016/j.biortech.2017.09.074.
31. Kumari, M.; Ghosh, P.; Thakur, I.S. Landfill leachate treatment using bacto-algal co-culture: An integrated approach using chemical analyses and toxicological assessment. *Ecotoxicol. Environ. Saf.* **2016**, *128*, 44–51, doi:10.1016/j.ecoenv.2016.02.009.
32. Škufca, D.; Prosenc, F.; Bulc, T.G.; Heath, E. Removal and fate of 18 bisphenols in lab-scale algal bioreactors. *Sci. Total Environ.* **2021**, 149878, doi:10.1016/j.scitotenv.2021.149878.
33. Watabe, Y.; Kondo, T.; Imai, H.; Morita, M.; Tanaka, N.; Hosoya, K. Reducing Bisphenol A Contamination from analytical procedures to determine ultralow levels in environmental samples using automated HPLC microanalysis. *Anal. Chem.* **2004**, *76*, 105–109, doi:10.1021/ac0301595.
34. Maadane, A.; Merghoub, N.; El Mernissi, N.; Ainane, T.; Amzazi, S. Antimicrobial activity of marine microalgae isolated from Moroccan coastlines. *J. Microbiol. Biotechnol. Food Sci.* **2017**, *6*, 1257–1260, doi:10.15414/jmbfs.2017.6.6.1257-1260.
35. Wang, S.; Said, I.H.; Thorstenson, C.; Thomsen, C.; Ullrich, M.S.; Kuhnert, N.; Thomsen, L. Pilot-scale production of antibacterial substances by the marine diatom *Phaeodactylum tricornutum Bohlin*. *Algal Res.* **2018**, *32*, 113–120, doi:10.1016/j.algal.2018.03.014.
36. Desbois, A.P.; Walton, M.; Smith, V.J. Differential antibacterial activities of fusiform and oval morphotypes of Phaeodactylum tricornutum (Bacillariophyceae). *J. Mar. Biol. Assoc. United Kingdom* **2010**, *90*, 769–774, doi:10.1017/S0025315409991366.
37. Kim, B.-H.; Ramanan, R.; Cho, D.-H.; Oh, H.-M.; Kim, H.-S. Role of Rhizobium, a plant growth promoting bacterium, in enhancing algal biomass through mutualistic interaction. *Biomass and Bioenergy* **2014**, *69*, 95–105, doi:10.1016/j.biombioe.2014.07.015.
38. Mujtaba, G.; Lee, K. Treatment of real wastewater using co-culture of immobilized Chlorella vulgaris and suspended activated sludge. *Water Res.* **2017**, *120*, 174–184, doi:10.1016/j.watres.2017.04.078.
39. Cho, D.H.; Ramanan, R.; Heo, J.; Lee, J.; Kim, B.H.; Oh, H.M.; Kim, H.S. Enhancing microalgal biomass productivity by engineering a microalgal-bacterial community. *Bioresour. Technol.* 2015, *175*, 578–585.
40. Bister, N.; Pistono, C.; Huremagic, B.; Jolkkonen, J.; Giugno, R.; Malm, T. Hypoxia and extracellular vesicles: A review on methods, vesicular cargo and functions. *J. Extracell. Vesicles* **2020**, *10*, doi:10.1002/jev2.12002.
41. Yarana, C.; St. Clair, D. Chemotherapy-Induced Tissue Injury: An insight into the role of extracellular vesicles-mediated oxidative stress responses. *Antioxidants* **2017**, *6*, 75, doi:10.3390/antiox6040075.
42. Abramowicz, A.; Widłak, P.; Pietrowska, M. Different Types of cellular stress affect the proteome composition of small extracellular vesicles: A mini review. *Proteomes* **2019**, *7*, 23, doi:10.3390/proteomes7020023.
43. Prosenc, F.; Piechocka, J.; Škufca, D.; Heath, E.; Griessler Bulc, T.; Istenič, D.; Buttiglieri, G. Microalgae-based removal of contaminants of emerging concern: Mechanisms in *Chlorella vulgaris* and mixed algal-bacterial cultures. *J. Hazard. Mater.* **2021**, *418*, 126284, doi:10.1016/j.jhazmat.2021.126284.
44. European Commission A new circular economy action plan for a cleaner and more competitive Europe 2020, 20.
45. García-Galán, M.J.; Arashiro, L.; Santos, L.H.M.L.M.; Insa, S.; Rodríguez-Mozaz, S.; Barceló, D.; Ferrer, I.; Garfí, M. Fate of priority pharmaceuticals and their main metabolites and transformation products in microalgae-based wastewater treatment systems. *J. Hazard. Mater.* **2020**, *390*, 121771, doi:10.1016/j.jhazmat.2019.121771.
46. Škufca, D.; Kovačič, A.; Prosenc, F.; Griessler Bulc, T.; Heath, D.; Heath, E. Phycoremediation of municipal wastewater: Removal of nutrients and contaminants of emerging concern. *Sci. Total Environ.* **2021**, *782*, 146949, doi:10.1016/j.scitotenv.2021.146949.
47. Cooper, M.B.; Smith, A.G.; Paszkowski, U.; Scott, B. Exploring mutualistic interactions between microalgae and bacteria in the omics age This review comes from a themed issue on Biotic interactions Edited by. *Curr. Opin. Plant Biol.* 2015, *26*, 147–153.
48. Kouzuma, A.; Watanabe, K. Exploring the potential of algae/bacteria interactions. *Curr. Opin. Biotechnol.* **2015**, *33*, 125–129, doi:10.1016/j.copbio.2015.02.007.
49. Woith, E.; Fuhrmann, G.; Melzig, M.F. Extracellular vesicles—connecting kingdoms. *Int. J. Mol. Sci.* **2019**, *20*, 5695, doi:10.3390/ijms20225695.
50. Škufca, D.; Kovačič, A.; Bulc, T.G.; Heath, E. Determination of 18 bisphenols in aqueous and biomass phase of high rate algal ponds: development, validation and application. *Chemosphere* **2021**, 129786, doi:10.1016/j.chemosphere.2021.129786.
51. ChemAxon Marvin 2019.
52. R Core Team R: A language and environment for statistical computing. 2020.
53. RStudio Team RStudio: integrated development for R. *RStudio, Inc., Boston, MA URL http//www. rstudio. com* 2020.
54. Wickham, H.; Averick, M.; Bryan, J.; Chang, W.; McGowan, L.; François, R.; Grolemund, G.; Hayes, A.; Henry, L.; Hester, J.; et al. Welcome to the Tidyverse. *J. Open Source Softw.* **2019**, *4*, 1686, doi:10.21105/joss.01686.

 doi:10.20944/preprints202206.0244.v1

55. Dragulescu, A.; Arendt, C. xlsx: Read, Write, Format Excel 2007 and Excel 97/2000/XP/2003 Files 2020.
56. Kassambara, A. rstatix: Pipe-Friendly Framework for Basic Statistical Tests 2020.